



## Linking Experimental Characterization and Computational Modeling of Grain Growth in Al-Foil

MELIK C. DEMIREL

*Carnegie Mellon University, Department of Materials Science & Engineering, PA, USA; Theoretical Division, T-1, Los Alamos National Laboratory, NM, USA*

ANDREW P. KUPRAT, DENISE C. GEORGE AND GALEN K. STRAUB

*Theoretical Division, T-1, Los Alamos National Laboratory, NM, USA*

ANTHONY D. ROLLETT

*Carnegie Mellon University, Department of Materials Science & Engineering, PA, USA*

**Abstract.** Experimental results on grain boundary properties and grain growth obtained using the Electron Backscattered Diffraction (EBSD) technique are compared with the Finite Element simulation results of an Al-foil with a columnar grain structure. The starting microstructure and grain boundary properties are implemented as an input for the three-dimensional grain growth simulation. In the computational model, minimization of the interface energy is the driving force for the grain boundary motion. The computed evolved microstructure is compared with the final experimental microstructure, after annealing at 550°C. Good agreement is observed between the experimentally obtained microstructure and the simulated microstructure. The constitutive description of the grain boundary properties was based on a 1-parameter characterization of the variation in mobility with misorientation angle.

**Keywords:** grain boundaries, finite element, simulation, mobility, microevolution

### Introduction

Computational modeling and experimental characterization can be linked to study the interface properties and microstructural evolution of materials. However, new experimental data is needed for the comprehensive understanding of the kinetics of grain evolution. Grain boundary energy and mobility can be extracted with the measurement of the geometry of triple junctions between grain boundaries [1]. Experimental results on grain boundary properties that are obtained from EBSD technique can be used to simulate the topological changes in grain boundary motion.

Simulation [2, 3], theory [4], and the experimental observation [5] of grain boundary evolution of

three-dimensional microstructures have been studied by several authors in the literature. A new technique for three-dimensional grain growth simulations was introduced by Kuprat [6]; this method utilizes gradient-weighted moving finite elements (GWMFE) [7] combined with algorithms for performing topological reconnections on the evolving mesh [8]. In this model, minimization of the interface energy is the main driving force for the grain boundary motion. Interface motion is assumed to obey a linear relation ( $v = \mu\kappa$ ) where  $\mu$  is reduced mobility,  $v$  is the velocity, and  $\kappa$  is the curvature of the grain boundary. An important verification of the model is that the expected power law dependence of growth kinetics is obtained [9]. The gradient in mobility has a major effect on the growth process. In this paper, the orientation

dependence of the boundary mobility is introduced in order to break the symmetry in GWMFE simulations. With the same simulation technique, both normal and abnormal grain growth in three-dimensions can be studied.

In the following section, a brief summary of experimental details is presented. This is followed by results from GWMFE simulation, then comparison with annealing experiment, and ending with a discussion and conclusion.

### Experimental Procedure

The samples, which have  $1 \times 1 \text{ cm}^2$  lateral dimensions and  $120 \text{ }\mu\text{m}$  thickness, were cut from 99.98% pure Al foil. The starting microstructure was polycrystalline and annealed in a horizontal tube furnace at a temperature of  $550^\circ\text{C}$  for 9 hours in a  $\text{N}_2$  environment. Under these conditions, a thin oxide layer is always present on the foil surfaces which prevents thermal grooves from forming along grain boundaries. After annealing, the specimen was quickly removed from the furnace and quenched under water, then mounted on a glass slide. The sample was then electro-polished at room temperature for 60 seconds with a solution of 730 ml ethanol, 100 ml ethylene glycol monobutylether, 78 ml perchloric acid, and 90 ml distilled water. A strong cube texture,  $\{100\}\langle 001 \rangle$ , was observed after the annealing, with a small number of grains deviating from cube texture. In order to locate the scanning area, microhardness indents were used. A second annealing for 20 minutes at  $550^\circ\text{C}$ , under the same conditions, was performed to generate the final microstructure.

A secondary electron image was recorded from the surface of the crystal and the grain morphology obtained by applying the Gabor Wavelet [10] image-processing algorithm, which detects the boundaries. The orientation information was extracted from EBSD patterns using standard EBSD methods [11]. EBSD scans were performed in beam control mode on the Al foil on an XL-40 Philips FEG Scanning Electron Microscope. A 52 mm diameter phosphor scintillation screen was used to observe the EBSD patterns, and the working distance (sample surface to gun tip) was fixed throughout the data acquisition process. Scan areas of  $800 \times 800 \text{ }\mu\text{m}^2$  with a three- $\mu\text{m}$  step size were used. It is important to note that the scan size was chosen so as to minimize the possible errors and accurately measure orientation in the scan plane [12].

### Simulation

As in [6], in the GWMFE method, interfaces are represented as parameterized piecewise linear surfaces:

$$\mathbf{x}(s_1, s_2) = \sum_{\text{nodes } j} \alpha_j(s_1, s_2) \mathbf{x}_j$$

Here,  $(s_1, s_2)$  is the surface parameterization, the sum is over the  $N$  interface nodes,  $\alpha_j(s_1, s_2)$  is the piecewise linear basis function (“hat function”) which is unity at node  $j$  and zero at all other interface nodes, and  $\mathbf{x}_j = (x_j^1, x_j^2, x_j^3)$  is the vector position of node  $j$ . We have that

$$\dot{\mathbf{x}}(s_1, s_2) = \sum_j \alpha_j(s_1, s_2) \dot{\mathbf{x}}_j$$

is the velocity of the surface at the point  $x(s_1, s_2)$  (based upon linear interpolation of node velocities) and

$$v_n = \dot{\mathbf{x}}(s_1, s_2) \cdot \hat{\mathbf{n}} \quad (\hat{\mathbf{n}} \text{ is local surface normal})$$

So

$$v_n = \sum_j (\hat{\mathbf{n}} \alpha_j) \cdot \dot{\mathbf{x}}_j \quad (1)$$

In effect, we have that the  $3N$  basis functions for  $v_n$  are equal to  $n_k \alpha_j$ , where  $\hat{\mathbf{n}} = (n_1, n_2, n_3)$ . These basis functions are discontinuous piecewise linear, since the  $n_k$  are piecewise constant.

The Gradient-Weighted Moving Finite Element method is to minimize

$$\int (v_n - \mu \sigma K)^2 dS \quad (2)$$

over all possible values for the derivatives  $\dot{x}_i$ . (The integral is over the surface area of the interfaces). We thus obtain

$$\begin{aligned} 0 &= \frac{1}{2} \frac{\partial}{\partial \dot{x}_i^k} \int (v_n - \mu \sigma K)^2 dS \quad 1 \leq k \leq 3 \quad 1 \leq i \leq N \\ &= \int (v_n - \mu \sigma K) n_k \alpha_i dS \end{aligned}$$

Using (1), we obtain a system of  $3N$  ODE’s:

$$\left[ \int \hat{\mathbf{n}} \hat{\mathbf{n}}^T \alpha_i \alpha_j dS \right] \dot{x}_j = \int \mu \sigma K \hat{\mathbf{n}} \alpha_i dS$$

or

$$C(x) \dot{x} = g(x) \quad (3)$$

where  $\mathbf{x} = (x_1^1, x_1^2, x_1^3, x_2^1, \dots, x_N^3)^T = (\mathbf{x}_1, \mathbf{x}_2, \dots, \mathbf{x}_N)^T$  is the  $3N$ -vector containing the  $x$ ,  $y$ , and  $z$  coordinates of all  $N$  interface nodes,  $\mathbf{C}(\mathbf{x})$  is the matrix of inner products of basis functions, and  $\mathbf{g}(\mathbf{x})$  is the right-hand side of inner products involving surface curvature. Since  $\hat{\mathbf{n}}\hat{\mathbf{n}}^T$  is a  $3 \times 3$  matrix, it is clear that  $\mathbf{C}(\mathbf{x})$  has a  $3 \times 3$  block structure. As explained in [6], the inner products involving curvature can equivalently be viewed as arising from a surface tension of magnitude  $\mu$  on each of the planar triangular cells of our discretization of the interfaces. This leads to the satisfaction of the Herring condition at triple lines.

The system of ODE's (3) is solved with an implicit second order backwards difference variable time-step ODE solver [6]. We use generalized minimal residual (GMRES) iteration [15] with block-diagonal preconditioner to solve the linear equations arising from the Newton's method. More details appear in [6]

To simulate the grain structure evolution, an area of  $500 \times 500 \mu\text{m}^2$  was chosen from the scanned experimental microstructure. It is assumed that the grains are columnar in nature and as such, their boundaries are perpendicular to the surface [16]. Hence, the grain boundary structure on the section plane is extruded in the third (thickness) direction to create the three dimensional mesh. In the initial configuration, the microstructure consists of 26 grains, which were used to construct a three-dimensional finite element mesh of 4328 tetrahedral elements in which the mesh lines conformed to the grain boundaries. Each grain is meshed independently and combined with LAGRIT [13] mesh generation software. The initial lattice orientation for each grain is then assigned based on the EBSD measurements. The total volume of the structure is kept constant during the simulation and exterior boundaries are assumed to be quasi periodic. The GWMFE method minimizes the function,  $\int (v - \mu\kappa)^2 dA$  over all possible values of  $dx/dt$  values, where  $A$  is the surface area,  $x$  is the vector containing coordinates of all interface nodes, and  $t$  is the explicit time. All other details related to GWMFE method can be found in reference [6]. The GWMFE method solves an ordinary differential equation, where computational time scales with the number of tetrahedral elements in the simulation box. In an SGI-O2/R10000, our simulations took approximately 10 minutes of CPU time.

Anisotropy of the model is introduced by a single parameter dependence in the grain boundary mobility. In the calculations, the relative mobility in columnar Al-foil depends on misorientation angle and is low for

Table 1. Experimentally measured relative mobility values of each grain interface.

Misorientation angle (degree)	Relative mobility values	Grain numbers (see Fig. 1) for each grain boundary
<3	0.03239	3-4 4-7 5-17 7-4 9-8 11-9 25-21
3-4	0.00355	2-9 5-6 5-16 7-9 13-23 15-21 19-20 19-26
4-5	0.037287	2-7 4-6 6-16 9-13 12-13 21-26 25-26
5-6	0.0239	2-10 3-7 6-14 15-16 15-19 25-24
6-7	0.029	6-8 7-8 12-9 13-14 15-18 16-17 19-18
7-8	0.005728	6-15
8-9	0.00934	6-7
9-10	0.0107	9-10 15-20 23-24
10-11	0.05033	24-26
11-12	0.254698	14-21
12-13	0.282448	14-9
13-15	0.404045	1-2 1-10 1-11 8-14 13-22 14-15 14-22 22-21
>15	0.8279	22-25 23-22 24-22

small misorientations but undergoes a sharp transition to high mobilities between ten and fifteen degrees misorientation [13]. It is assumed that capillarity is the only driving force for boundary migration. Note that relative mobility values are calculated based on the low angle boundaries and all high angle boundaries are considered to have uniform (high) mobility. The local equilibrium condition at triple junctions is determined by the grain boundary energies. Relative boundary energies and mobilities were extracted through a statistical/multiscale analysis [17] and are given in Table 1 for the pre-annealed microstructure. The variation in energy was not considered in these simulations, however. The first column in Table 1 indicates the relative grain boundary mobility. The second column denotes the grains that have an interface with the relative mobility value in the initial microstructure.

## Results

The simulated results of microstructure evolution show large differences between isotropic and anisotropic

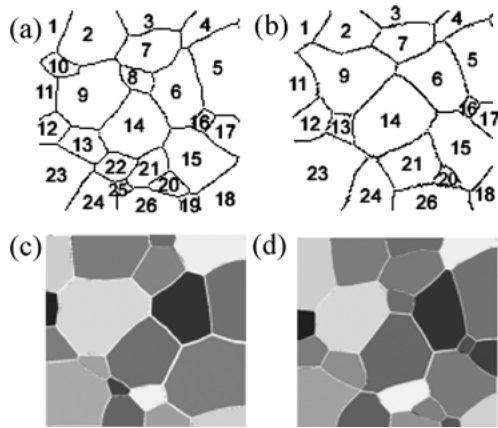


Figure 1. Comparison of experiment and predicted grain morphology: Experimentally obtained microstructure (a) before annealing (500  $\mu\text{m}$  by 500  $\mu\text{m}$ ) (b) after annealing, and simulated final microstructure (top view) with (c) isotropic properties (d) anisotropic properties.

dependence in terms of grain morphology. It was found that when starting with identical initial microstructures, varying the mobility dependence caused significant differences in the final microstructure. Isotropic (i.e., mobility is constant and equal at all boundaries) and anisotropic simulation results are contrasted in Fig. 1. In the isotropic case, Fig. 1(c), the final microstructure has preserved the larger grains, but the smaller grains have disappeared, as would be expected from having fewer than six sides. In contrast to the simulation with isotropic properties, examination of the experimental microstructure, Fig. 1(b), reveals that four sided grain number 16 did not disappear after annealing. Additionally, some of the small grains (number 13 and 20) shrank but preserved their identities. In addition to these grains, there are also some important topological changes in the final annealed structure. Grains numbered 8, 10, 19 vanished completely, and numbers 21, 22, 25 coalesced into grain number 21. As shown in Fig. 1(d), for the case of anisotropic simulation, grain topology is correctly predicted except for the grain number 8.

Microstructures moving under curvature driven motion obey Von Neumann-Mullins' law [18], which is given by  $dA/dt = \int (v) dS$ , where  $A$  is the area of the grain, and  $v$  is the normal velocity (positive when vector points outward), and the integral is taken over the arc-length of grain boundary. For an isotropic mobility and energy, grains, which have sides bigger than six, will grow and those with fewer than six will disappear. For

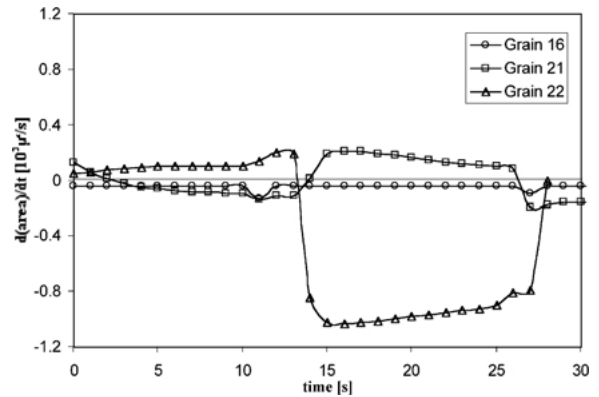


Figure 2. Rate of change in the area of grains is determined by the anisotropy (mobility, and energy dependence of misorientation) of the boundaries.

anisotropic case, however, this is not always true. The rate of change in the area of three specific grains (number 16, 21 and 22) is shown in Fig. 2. Grain number 16, which has four sides, has an approximately constant rate that is slightly negative as expected. On the other hand, grain number 22, which has six sides and a negative rate of change of area, vanishes completely (Fig. 1(d)) at the end of the simulation. Grain number 21 also has six sides and alternates between positive and negative growth rates. At the end of the simulation it has lost one side and its growth rate has become negative, in agreement with the von Neumann-Mullins' law.

## Discussions and Conclusion

The comparison between the experiment and computed results provides important details related to grain evolution. A strong similarity is observed between growth experiments and anisotropic three-dimensional GWMFE simulations. It is clear from the simulation results that anisotropy in the grain boundary energy and mobility has a major effect on growth process and the growth is driven by these parameters. Combining the three dimensional grain growth simulations results with experimental outputs will provide a computational tool for the discovery of some new methods to design meso-structures.

Absolute grain boundary mobility values were measured by Gottstein et al. in Aluminum bi-crystals and reduced mobilities (i.e. the product of mobility with energy) of order  $10^{-8}$  to  $10^{-7}$   $\text{m}^2 \cdot \text{s}^{-1}$  for

two similar types of high angle boundary and various purities were obtained [14]. For curvatures of about  $100 \mu\text{m}^{-1}$  (i.e., boundary interface between grain 1 and 2) suggest migration rates of approximately  $v = \mu\sigma\kappa = 5 \cdot 10^{-8} 100 = 5 \mu\text{m}\cdot\text{s}^{-1}$ . These migration rates are high when compared to the estimated migration rates in the experiment ( $0.1 \mu\text{m}\cdot\text{s}^{-1}$ ). We note, however, that the purity of the material used in the bi-crystal experiments was significantly higher than that in our experiments. For the comparison of simulation times with experiment, these values can be used to estimate the migration distance during the annealing at various temperatures.

We conclude that the present simulation method verified the experimentally determined microstructural evolution. The simulation model was an idealized grain growth case, and future extensions may be made to systems that are more complex and these further studies should foster a more comprehensive understanding of grain growth. Extension of this work to a five-parameter dependence of grain boundary energy and mobility is in preparation.

### Acknowledgments

This work was supported by the MRSEC program of NSF under award number DMR-0079996 and Department of Energy under Contract W-7405-ENG-36 and completed during visits supported by the Computational Materials Science Network, US Department of Energy.

### References

1. B.L. Adams, D. Kinderlehrer, W.W. Mullins, A.D. Rollett, and S. Ta'asan, *Scripta Materialia* **38**, 531 (1998).
2. M.P. Anderson, G.S. Grest, and D.J. Srolovitz, *Philosophical Magazine B* **59**, 293 (1989).
3. F. Wakai, N. Enomoto, and H. Ogawa, *Acta Materialia* **48**, 1297 (2000).
4. W.W. Mullins, *Acta Metallurgica* **37**, 2979 (1989).
5. D.J. Jensen, H.F. Poulsen, and T. Lorentzen, Plastic Deformation, Recrystallization and Internal Stresses studied by a new 3D X-Ray Microscope, MRS Fall'99 Meeting, Boston, MA, USA (1999).
6. A. Kuprat, *Siam J. Scientific Computing* **22**, 535 (2000).
7. N.N. Carlson and K. Miller, *Siam J. Scientific Computing* **19**, 766 (1998).
8. A. Kuprat, Los Alamos National Laboratory Report LA-UR-00-3475 (2000).
9. G.K. Straub, D.G. George, and A.P. Kuprat, Los Alamos National Laboratory Report LA-UR-00-1 (2000).
10. C.E. Shannon, *Proc. IRE* **10** (1949).
11. S.I. Wright, B.L. Adams, and K. Kunze, *Mat. Sci. & Eng. A* **160**, 229 (1993).
12. M.C. Demirel, A.P. Kuprat, D.C. George, B.S. El-Dasher, N.N. Carlson, G. K. Straub, and A.D. Rollett, *Proceedings of Materials Research Society Fall Meeting* (2000).
13. D. George, User Manual, <http://www.t12.lanl.gov/~lagrit/> (1995).
14. G. Gottstein, D.A. Molodov, and L.S. Shvindlerman, *Interface Science* **6**, 7 (1998).
15. Y. Saad and M.H. Schultz, *SIAM J. Sci. Stat. Comput* **7**, 856 (1986).
16. C.-C. Yang, A.D. Rollett, and W.W. Mullins, *Scripta Materialia*, in press.
17. D. Kinderlehrer, I. Livshits, S. Ta'asan, and D.E. Mason, Multiscale Reconstruction of Grain Boundary Energy from Microstructure, Twelfth International Conference on Textures of Materials, Montréal, Canada (1999).
18. W.W. Mullins, *J. Appl. Phys.* **27**, 900 (1956).